AFOSR-TR-95

0546

REPORT DOCUMENTATION PAGE

Public reporting burden for this collection of information is estimated to average 1 hour per response, including the time for reviewing instructions, searching existing data sources, gathering and maintaining the data needed, and completing and reviewing the collection of information. Send comments regarding this burden estimate or any other aspect of this collection of information, including suggestions for reducing this burden, to Washington Headquarters Services, Directorate for Information Operations and Reports, 1215 Jefferson Davis Highway, Suite 1204, Arlington, VA 22202-4302, and to the Office of Management and Budget, Paperwork Reduction Project (0704-0188), Washington, DC 20503.

1. AGENCY USE ONLY (Leave blank)	2. REPORT DATE	3. REPORT TYPE AND DATES COVERED
	12 May 1995	FNL.TECH.RPT: 1/9/91 - 31/3/95

4. TITLE AND SUBTITLE
(U) Rapid Concentration Measurements by Picosecond Time-Resolved Laser-Induced Fluorescence

5. FUNDING NUMBERS
PE - 61102F
PR - 2308
SA - BS
G - AFOSR 91-0365

6. AUTHOR(S)
G. B. King and N. M. Laurendeau

7. PERFORMING ORGANIZATION NAME(S) AND ADDRESS(ES)
Purdue University
West Lafayette, IN 47907-1288

8. PERFORMING ORGANIZATION REPORT NUMBER

9. SPONSORING/MONITORING AGENCY NAME(S) AND ADDRESS(ES)
AFOSR/NA
110 Duncan Ave., Suite B115
Bolling AFB DC 20332-0001

AUG 25 1995

10. SPONSORING/MONITORING AGENCY REPORT NUMBER
AFOSR-91-0365

11. SUPPLEMENTARY NOTES

12a. DISTRIBUTION/AVAILABILITY STATEMENT
Approved for public release; distribution is unlimited.

12b. DISTRIBUTION CODE

13. ABSTRACT *(Maximum 200 words)*

Measurements of probability density functions (PDFs) and power spectral densities (PSDs) are needed to characterize minor species concentrations in turbulent flames. Current techniques can be used to measure PDFs, but they have limited ability to measure PSDs because they cannot monitor a time-series of the number density fluctuations. This report described the development of a new strategy, picosecond time-resolved laser-induced fluorescence (PITLIF), which can possibly be used to obtain measurements of minor species concentrations in flames on the time scale of turbulence. PITLIF was demonstrated by seeding sodium into a laminar $H_2/O_2/Ar$ nonpremixed flame and monitoring both the integrated fluorescence signal and fluorescence signal and fluorescence lifetime. PITLIF was also used to determine hydroxyl concentrations in laminar $CH_4/O_2/N_2$ flames. The quenching environment was monitored with real-time sampling, and thus the necessary quenching rate coefficient was obtained on the time scale of turbulence (348 μs). Fluorescence lifetimes of OH were also measured at different equivalence ratios by using the equivalent-time sampling technique. These results compared favorably with predicted lifetimes based on relevant quenching cross-sections and calculated species concentrations.

19950824 191

14. SUBJECT TERMS
Laser-Induced Fluorescence
Time-Resolved Fluorescence
Concentration Measurements
Turbulent Flames

DTIC QUALITY INSPECTED 5

15. NUMBER OF PAGES
19

16. PRICE CODE

17. SECURITY CLASSIFICATION OF REPORT	18. SECURITY CLASSIFICATION OF THIS PAGE	19. SECURITY CLASSIFICATION OF ABSTRACT	20. LIMITATION OF ABSTRACT
Unclassified	Unclassified	Unclassified	UL

RAPID CONCENTRATION MEASUREMENTS BY PICOSECOND TIME-RESOLVED LASER-INDUCED FLUORESCENCE

Final Report
Air Force Office of Scientific Research
Grant No. AFOSR-91-0365
September 1, 1991 - March 31, 1995

Galen B. King and Normand M. Laurendeau
School of Mechanical Engineering
Purdue University
West Lafayette, IN 47907

Abstract

Measurements of probability density functions (PDFs) and power spectral densities (PSDs) are needed to characterize minor species concentrations in turbulent flames. Current techniques can be used to measure PDFs, but they have limited ability to measure PSDs because of the difficulties associated with obtaining a time-series for the fluctuations in number density. This report described the development of a new strategy, picosecond time-resolved laser-induced fluorescence (PITLIF), which can possibly be used to obtain measurements of minor species concentrations in flames on the time scale of turbulence. PITLIF was demonstrated by seeding sodium into a laminar $H_2/O_2/Ar$ nonpremixed flame and monitoring both the integrated fluorescence signal and the fluorescence lifetime. PITLIF was also used to determine hydroxyl concentrations in laminar $CH_4/O_2/N_2$ flames. The quenching environment was monitored with real-time sampling, and thus the necessary quenching rate coefficient was obtained on the time scale of turbulence (348 μs). Fluorescence lifetimes of OH were also measured at different equivalence ratios by using the equivalent-time sampling technique. These results compared favorably with predicted lifetimes based on relevant quenching cross-sections and calculated species concentrations.

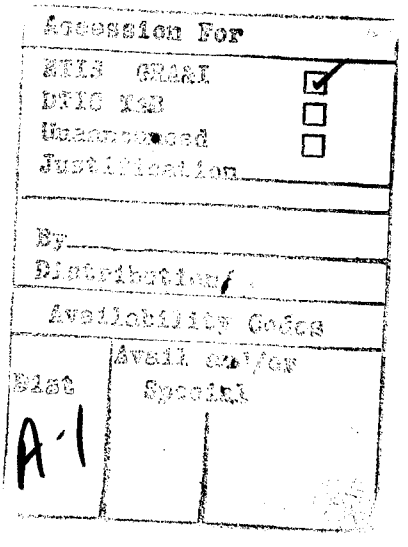

1. RESEARCH OBJECTIVES

The ability to make accurate, spatially and temporally resolved concentration measurements in turbulent flames is an important step in designing cleaner, more efficient combustion devices. Turbulence implies irregular fluctuations in flow variables such as velocity or concentration which are best described statistically using probability density functions (PDFs) and power spectral densities (PSDs). The PDFs and PSDs can then be used for validation of theoretical turbulence and combustion models [1]. Simultaneous measurement of both PDFs and PSDs is particularly challenging for minor species concentrations. Such a measurement is the primary goal of this research.

Laser-induced fluorescence (LIF) possesses the spatial and temporal resolution necessary to monitor radical concentrations in turbulent, reacting flows. When using LIF to measure number density, the excited atom or molecule may return to its ground state via two paths: (1) the emission of a photon (fluorescence), or (2) collision with another atom or molecule (quenching) [2]. Thus, the quenching environment must either be monitored or the dependence of the fluorescence signal on collisional quenching must be eliminated to determine concentrations from fluorescence signals.

The present work focuses on the application of a new diagnostic technique, picosecond time-resolved laser-induced fluorescence (PITLIF), to the measurement of the number density of sodium and hydroxyl (OH) in laminar flames. While most practical combustion devices involve turbulent flames, laminar flames are studied here because they provide a well-controlled, steady-state environment which allows the OH results to be more easily compared with existing computer models. By monitoring laminar flames, we also demonstrate the potential of PITLIF to account for variations in the quenching environment on the time scale of turbulence.

In the PITLIF method, the local quenching environment is monitored via a high-bandwidth channel (0-2 GHz) capable of resolving the individual temporal decays in the fluorescence signal. Hence, the integrated signal monitored by a parallel low-bandwidth channel can be corrected for quenching rate variations by employing the measured fluorescence lifetimes. A mode-locked laser with a rapid pulse repetition rate (82 MHz or 4 MHz) is used as the excitation source. We have demonstrated this technique by separately obtaining low- and high-bandwidth fluorescence data for sodium seeded into a flame and then correcting the former by averaging the latter over many temporal waveforms in an equivalent-time sampling mode. We have confirmed our ability to obtain the quenching rate coefficient of sodium on the time scale of turbulence via real-time sampling of the high-bandwidth fluorescence signal. We also report on equivalent- and real-time measurements of OH fluorescence lifetimes, as well as on our ability to measure OH number densities. We thus demonstrate concentration measurements of a naturally-occurring minor species for a variety of atmospheric flame conditions using the fluorescence induced by a picosecond laser excitation source.

2. RESEARCH ACCOMPLISHMENTS

2.1 Sodium Measurements

To verify operation of the PITLIF technique, we have employed the instrument to measure fluorescence fluctuations of sodium seeded into a laminar $H_2/O_2/Ar$ nonpremixed flame. In this case, the fluctuations in atomic sodium originate from the atomization process used to seed

sodium into the flame. However, by employing this simple laminar flame, we are able to demonstrate the utility of the technique for studying important combustion radicals in turbulent systems. The instrument will ultimately be useful in flames for which turbulent interactions are largely responsible for the number density fluctuations.

A schematic diagram of the experimental apparatus for the sodium measurements is shown in Fig. 1. The gases were burned in a concentric tube burner which consists of a circular port surrounded by two annular ports. The sodium was introduced by atomization of a NaCl solution into the oxidizer stream. The laser source is a Spectra-Physics 375B broadband dye laser with Rhodamine 6G dye synchronously pumped by a mode-locked frequency-doubled Spectra-Physics Series 3000 Nd:YAG laser. The dye laser output is tuned to 589.0 nm to excite the $3S_{1/2} \rightarrow 3P_{3/2}$ transition in atomic sodium using a two-plate lyot filter and étalon. The laser system delivers a series of mode-locked laser pulses with a repetition rate of 82 MHz. The laser beam is chopped by an optical chopper operated at 4 kHz to allow for synchronous detection, thus eliminating any signal from flame emission. Fluorescence emission is collected perpendicular to the beam axis and focused onto a photomultiplier tube (PMT) designed for fast response. For the low-bandwidth measurements, the output of the PMT is directed into a low-pass filter which provides amplification and filters out the individual temporal decays induced by the laser pulses. The output of the low-pass filter is then directed into a lock-in amplifier which is triggered from the chopper. The output of the lock-in amplifier is digitally sampled by a data acquisition system.

For the high-bandwidth measurements, the output of the PMT is directed to a digital signal analyzer (DSA). The DSA can be operated in a real-time or an equivalent-time sampling mode. In the real-time mode, the PMT current is sampled in a continuous fashion. In the equivalent-time mode, the DSA operates as a sampling oscilloscope in which many sweeps are interleaved to obtain a temporal record of a repetitive waveform. Both methods require triggering from the pulse source (see Fig. 1). The data collected with either method were then downloaded to the microcomputer for analysis.

2.1.1 Low-Bandwidth Measurements

Figure 2(a) displays PDFs of LIF intensity for various locations in the nonpremixed flame. The differences in LIF intensity with axial (x-direction) and radial (r-direction) position are expected due to the fact that sodium is diffused into the flame zone from the external coflowing O_2/Ar flow. The wide tails of the PDFs are due to the fluctuations in sodium concentration which result from the atomization process. A clear difference exists in the two PDFs at x = 3 mm. At r = 3 mm, which is near the flame edge, the LIF signal exhibits a wide range of intensity fluctuations. At r = 0 mm, a large spike of low-intensity values is found, thus indicating little diffusion of sodium to the center of the flame at this low axial location. At x = 10 mm on the other hand, sodium is well distributed across the flame radius. Local PSDs are presented in Fig. 2(b) for two different axial locations in the flame. These PSDs are normalized by the mean-square of the LIF intensity fluctuations. A larger contribution by high frequency fluctuations is found at the lower axial position. Significant damping of the spectral energy at the higher frequencies occurs between x = 3 mm and x = 10 mm.

2.1.2 High-Bandwidth Measurements

Initial studies of the high-bandwidth portion of the instrument were performed using the equivalent-time mode of the DSA. Each laser pulse induces a fluorescence decay which is depicted in Fig. 3(a). The instrument response based on scattering from repetitive laser pulses is also included in Fig. 3(a). The waveforms in Fig. 3(a) were smoothed using the DSA 602A digital n-pole Bessel filter with a risetime of 700 ps after averaging approximately 500 equivalent-time waveforms. Since the instrument response time is on the same order of magnitude as the lifetime of the decay, a convolute-and-compare technique must be utilized to obtain the fluorescence lifetime. This technique iteratively convolves the measured instrument response with an assumed form of the decay until it matches the measured decay within prescribed limits [3].

Because the equivalent-time mode requires an acquisition time greater than the time scale of turbulence, it is only suitable for measuring the average quenching environment at a specific location in the flame. To demonstrate that the PITLIF instrument can monitor turbulent fluctuations, we now show that the quenching environment can be monitored on the time scale of turbulence. To simulate real-time acquisition without re-arming, successive real-time data samples were combined via a trigger from the laser mode locker. The data is transferred from the DSA to a PC and processed in software. A record of the PMT current is analyzed by dividing it into data ranges, the temporal width of the ranges being equal to the inverse of the laser repetition rate. Each of these data ranges is divided into bins with a temporal width equal to the inverse of the acquisition rate. The data points are accumulated to generate a composite decay similar to the procedure described by Nowak et al. [4]. At the acquisition rate of 1 Gsample/s, the maximum number of points that can be acquired before the DSA must re-arm is 20,464. The resulting 20.5 μs sampling time was not sufficient to adequately resolve the decay from the background flame emission. By obtaining 20 files at 1 Gsample/s (for a total sampling time of 409 μs), we were able to reconstruct a meaningful fluorescence decay. Figure 3(b) displays the corresponding real-time excitation pulse and fluorescence decay. While the equivalent-time data has a point density 20 times that of the real-time data, the curves are qualitatively and quantitatively similar.

A quantitative comparison of equivalent-time and real-time lifetimes was conducted by measuring the fluorescence lifetime via each method as a function of position in the flame. The favorable results are shown in Fig. 4. The error bars ($\pm 2\sigma$) in Fig. 4 were determined from a statistical analysis using 20 trials of each method at r = 2 mm, x = 10 mm in the flame. The mean (μ) and sample standard deviation (σ) of the fluorescence lifetimes were calculated for both groups of 20 trials, and the fractional errors were calculated as the standard deviation divided by the mean (μ/σ). The resulting fractional error was 0.100 for the equivalent-time method and 0.087 for the real-time method. These fractional errors are assumed to be independent of position in the flame.

Now that we have demonstrated the ability of the PITLIF instrument to capture the fluorescence decays on the time scale of turbulence, we will show how these results are used to correct the low-bandwidth data for quenching. As discussed earlier, the excited state lifetime is necessary to obtain the number density of the atom or molecule under study. The number density relative to that determined by calibration is

$$\frac{N_1^o}{N_{1,c}^o} = \left(\frac{\tau_c}{\tau}\right)\left(\frac{S_F}{S_{F,c}}\right) \qquad (1)$$

where the subscript c indicates the calibration condition, τ is the fluorescence lifetime, and S_F is the fluorescence signal. Figure 5 employs Eq. (1) to compare on a relative basis uncorrected sodium number densities with those corrected for quenching. The values are based on the mean intensity signals at the various locations in the flame. To demonstrate the effect of collisional quenching, the uncorrected value acquired at x = 10 mm, r = 0 mm was normalized to unity and all subsequent data were normalized with respect to this point. Similarly, all relative number densities corrected for quenching were normalized relative to the calibration value found at x= 10 mm, r= 0 mm. As seen in Fig. 5, the effect of collisional quenching on number density is non-uniform across the flame. Furthermore, the corrected radial profile is more consistent with the expected high level of sodium at r > 2 mm. Thus, local measurements of quenching are clearly vital for accurate number density measurements.

2.2 Hydroxyl Measurements

Following the sodium studies, we modified the laser and detection systems to allow us to excite and monitor hydroxyl (OH). For the OH measurements, the dye laser is operated in conjunction with a Spectra-Physics 344 cavity dumper, thus decreasing the laser repetition rate from 82 MHz to 4 MHz. The cavity dumper is used because it creates higher peak power, which increases the efficiency of the subsequent frequency-doubling process. The visible output of the cavity dumper is frequency doubled using a lithium iodate ($LiIO_3$) crystal. Fluorescence emission was collected perpendicular to the beam axis and focused onto the entrance slit of a 0.25-m monochromator which was centered at 309 nm. The spectral width of the detection system was 26 nm (assuming a negligible entrance slit width). For the LIF results reported in this work, the excitation line was the $Q_1(7)$ transition of the $A^2\Sigma^+ - X^2\Pi$ ($\upsilon'=0,\upsilon''=0$) system (λ = 308.9734 nm) [5].

Hydroxyl lifetimes were measured in flames produced by two different burner systems. The first system utilized a nonpremixed square 25mm x 25mm Hencken burner; it is composed of a bundle of stainless steel tubing, each tube for the fuel flow being surrounded by six tubes for the flow of an oxidant/diluent mixture. Methane was used as the fuel. Oxygen diluted with N_2 was used as the oxidant, with a volumetric dilution ratio for N_2 to O_2 of 3.76. The total flow rate of the fuel plus the oxidant/diluent mixture was 10 L/min. Rapid diffusion occurs near the burner surface; hence it can be assumed that the mixture in the center of the burner is at the same stoichiometry as the input gases. The other burner utilized was a premixed water-cooled, sintered-bronze, 6-cm diameter McKenna burner, which used a similar mixture of CH_4-O_2-N_2. The dilution ratio was again 3.76 but the total flow rate was increased to 17 L/min. Unless otherwise stated, the OH fluorescence signal was again monitored 5 mm above the center of the burner surface.

2.2.1 High-Bandwidth Measurements

The Hencken burner was operated at equivalence ratios (ϕ) in the range 1.0-1.5. A typical fluorescence decay obtained 5 mm above the burner at ϕ = 1.0 is displayed in Fig. 6(a), along with the excitation pulse collected from laser scattering and the fit determined with the convolute-and-compare algorithm. The resulting lifetimes obtained 5 mm above the center of the Hencken burner are displayed in Fig. 7(a) for different equivalence ratios. Each point displayed on the figure represents the average of six trials, with the error bars representing the 95% confidence interval of the mean. The fluorescence lifetimes range from a maximum of 1.91 ± 0.07 ns at ϕ = 1.0 to a minimum of 1.66 ± 0.07 ns at ϕ = 1.5. Figure 7(a) indicates that the smallest lifetimes are observed for richer conditions.

The McKenna burner was operated at equivalence ratios in the range ϕ = 0.8 - 1.4. As in our study of the Hencken burner, Fig. 7(b) displays fluorescence lifetimes obtained via equivalent-time sampling versus equivalence ratio for the premixed McKenna burner. The fluorescence lifetimes range from a maximum of 1.84 ± 0.08 ns at ϕ = 0.8 to a minimum of 1.37 ± 0.05 ns at ϕ = 1.4. Similar to the data obtained with the Hencken burner, there is a noticeable decrease in lifetime with increasing equivalence ratio.

Figure 7(b) includes the fluorescence lifetime obtained from real-time measurements at stoichiometric conditions. The point at ϕ = 1.0 represents the average of 20 lifetimes obtained in the real-time mode for the McKenna burner, with the error bars representing the 95% confidence interval of the mean. The flame with ϕ = 1.0 was chosen for this investigation due to its relatively high SNR (~4). We have already demonstrated the viability of real-time fluorescence measurements for atomic sodium (see Fig. 4); thus, only one equivalence ratio was investigated for the case of OH.

Figure 6(b) shows a typical waveform obtained using real-time acquisition, including the excitation pulse and the fit determined through convolution. Seventeen files were acquired and combined to obtain a single lifetime, resulting in a total sampling time of 348 μs. The point density of 1 point/ns in Fig. 6(b) is limited by the inverse of the DSA sampling rate (1 Gsample/s). While the real-time fluorescence lifetimes exhibit more statistical scatter than the equivalent-time data (as evidenced by the acquisition of 20 lifetimes to obtain a reliable average), the average value agrees favorably with that obtained using equivalent-time sampling (see Fig. 7(b)).

At atmospheric pressure, the fluorescence lifetime τ (s) of hydroxyl is equivalent to the inverse of the quenching rate coefficient Q_{21} (s^{-1}). We have calculated the quenching rate coefficient for OH from

$$Q_{21} = \sum_i k_{Qi} n_i \qquad (2)$$

where k_{Qi} is the bimolecular quenching rate constant ($cm^3\ s^{-1}$) for the ith species and n_i is the number density of the ith species (cm^{-3}) [6]. The quenching rate constant for the ith species is related to its collisional cross-section σ_{Qi} (cm^2) by [6]

$$k_{Qi} = \bar{v}\sigma_{Qi}, \qquad (3)$$

where $\bar{v}$ (cm/s) is the mean relative velocity of the colliding species. The collisional cross-sections for all molecules considered in the calculations with the exception of N_2 were taken from tabulated best-fit coefficients given by Paul [7]. Experimentally, the collisional cross-section for N_2 is not accounted for by the 'harpooned' mechanism; thus, this value was calculated from the data given by Garland and Crosley [6]. The N_2 cross-section has been shown to be small, but quenching due to N_2 becomes significant because of the large amounts of N_2 in the flame. For the Hencken burner, the number densities required for Eq. (2) were obtained by assuming chemical equilibrium. However, to account for radiative and conductive heat losses, the predicted lifetimes shown in Fig. 7(a) were obtained by assuming temperatures both 100 K and 200 K less than the adiabatic flame temperature. Previous work has demonstrated that the measured temperature for a Hencken burner operated at stoichiometric to rich conditions is up to 200 K less than the adiabatic flame temperature [8].

Predictions of similar fluorescence lifetimes for the McKenna burner are shown in Fig. 7(b). In this case, the species number densities for the fluorescence lifetime calculations were obtained from the Sandia steady, laminar, 1-D, premixed flame code [9], while the temperatures for these calculations were obtained from radiation-corrected thermocouple measurements. The CHEMKIN-II computer program library [10] was used to process the reaction mechanism into a form which is appropriate for use by the Sandia flame code. The transport and thermodynamic properties were provided by two accompanying data bases [11, 12].

Figures 7(a) and (b) demonstrate the favorable agreement between the measurements and predictions of the fluorescence lifetime. The flame models for both burners show that the fluorescence lifetime decreases with increasing equivalence ratio, a trend which we also observed for the experimental results. In addition, the Hencken burner flames modeled at 200 K less than the adiabatic flame temperature exhibit excellent quantitative agreement with the measured fluorescence lifetimes. Figures 7(a) and (b) represent the first extensive comparisons between fluorescence lifetimes obtained experimentally in atmospheric flames and those obtained from computer modeling. The maximum deviation between the mean measured lifetimes and the lifetimes obtained from the 'harpooned' model was found for the McKenna burner flame at ϕ = 1.4. However, even for this flame condition, the modeling over-predicts the measured lifetime by only 13%.

Though the comparisons between the predicted and measured fluorescence lifetimes are quite good, there are several factors which could account for the observed discrepancies. These factors are generally related to the direct influence of temperature on both the modelled species number densities and collisional cross-sections. The consequent effect of a predicted temperature difference of 100 K on the fluorescence lifetimes is illustrated in Fig. 7(a). Unfortunately, obtaining accurate temperature measurements, especially near the burner surface, is particularly difficult for the Hencken burner. To model the species mole fractions for the McKenna burner, we used the temperature profile provided by the energy solution to the flame equations. Because this temperature profile does not account for radiative heat losses, it predicts higher post-flame temperatures than were obtained experimentally. For this reason, we used radiation-corrected thermocouple measurements (Pt/Pt-10%Rh) for calculation of the quenching environment. Thermocouple measurements might suffer from catalytic effects in the high-temperature flame

front, but such catalytic effects should be negligible 5 mm above the burner surface. There are very few experimental collisional data at elevated temperatures with which to test collisional quenching models. Thus, we must be cognizant of the uncertainty in the measured temperatures in this study and also the related uncertainty in the predictive capability of the quenching model at higher temperatures.

2.2.2 Low-Bandwidth Measurements

Low-bandwidth data were also obtained using the McKenna burner to demonstrate the ability of the PITLIF system to determine OH number densities. The low-bandwidth fluorescence signal was corrected for both laser power fluctuations (by monitoring the laser power with a radiometer) and background emission (via synchronous detection). Each low-bandwidth point presented is the result of averaging 10,000 samples acquired at 400 Hz. The flames probed with the low-bandwidth system were also investigated through computer modeling.

Figure 8 demonstrates the relative quenching-corrected hydroxyl number density at various equivalence ratios in the post-flame region. The LIF data uncorrected for quenching are included for the sake of comparison. The LIF signal is measured with the low-bandwidth system, and the corrected number densities are obtained via Eq. (1) for which the subscript c indicates the calibration condition at $\phi = 0.9$. The results of the kinetic modeling are also displayed in Fig. 8. The temperature profile required for the modeling was provided by solution of the energy equation.

Figure 8 shows that the quenching correction is rather minimal for the equivalence ratios investigated, as the OH lifetimes did not vary widely for this equivalence ratio range. The only point which differs significantly from the predictions is at stoichiometric conditions. Besides the higher experimental uncertainties involved with a measurement at $\phi = 1.0$, there is another possible reason for this particular difference. The average laser beam power was monitored after the beam passed through the flame, and thus it would be sensitive to laser absorption. To obtain the values graphed in Fig. 8, the average fluorescence signal is divided by the average laser power. The higher OH number density at stoichiometric conditions would increase laser absorption. Since laser absorption could decrease the measured laser power at $\phi = 1.0$, the normalized number density measurement at $\phi = 1.0$ might be enhanced compared to the actual number density.

Because of the uncertainty in the lifetime measurements, it is not evident that the quenching correction is necessary to improve the accuracy of the present OH number density measurements. However, we should expect larger deviations from stoichiometric conditions in nonpremixed flames. Barlow *et al.* [13] found that OH measurements in turbulent nonpremixed H_2-air flames required a 300% quenching correction for a mixture fraction (ξ) of 0.4. This quenching correction was based on comparisons to a calibration flame in a slightly lean Hencken burner. Unfortunately, lifetimes in richer flames were not monitored in our study due to the poor SNR at $\phi > 1.4$ (corresponding to $\xi > 0.076$ for the present $CH_4/O_2/N_2$ flame). A higher-powered picosecond pulsed laser would be required to monitor turbulent nonpremixed systems for which the mixture fraction varies widely.

In addition to the equivalence-ratio scan shown in Fig. 8, we measured the low-bandwidth fluorescence signal as a function of height above the burner for $\phi = 1.0$. The results are

displayed in Fig. 9. Because our lifetime measurements showed that the quenching environment is relatively constant with height above the burner for this flame, we did not correct the number densities for quenching as in Fig. 9. The results of the kinetic modeling are also displayed in Fig. 9. We again used the temperature profile obtained via the energy solution as provided by the kinetics modeling. While good agreement exists between the predicted and experimental results up to a height of 5 mm above the burner, the model predicts consistently higher number densities than were experimentally measured at greater heights. This deviation is likely due to the inability of the computer code to account for radiative heat losses. Such losses will decrease the temperature of the post-flame gases and thus decrease the relative OH concentration.

2.3 Conclusions

In conclusion, we have measured sodium and hydroxyl number densities using the fluorescence induced by a picosecond laser excitation source. The quenching environment can be experimentally monitored by employing fluorescence lifetimes obtained with the high-bandwidth channel of the PITLIF instrument. The LIF signal obtained via the low-bandwidth channel can then be corrected for variations in the quenching environment. The measured OH fluorescence lifetimes agree well with those predicted using the quenching cross-sections from Paul [7] and from Garland and Crosley [6]. We have also obtained OH lifetimes in a flame at an acquisition rate on the time scale of turbulence. Hence, the PITLIF technique should be applicable to the measurement of turbulent concentration fluctuations in reactive flows.

3. PUBLICATIONS AND PRESENTATIONS

(1) M. S. Klassen, B. D. Thompson, T. A. Reichardt, G. B. King, and N. M. Laurendeau, "Flame concentration measurements using picosecond time-resolved laser-induced fluorescence," *Combust. Sci. Tech.* **97**, 391 (1994).

(2) T. A. Reichardt, M. S. Klassen, G. B. King, and N. M. Laurendeau, "Real-time acquisition of laser-induced fluorescence decays," *Appl. Opt. 34,* 973 (1995).

(3) T. A. Reichardt, M. S. Klassen, G. B. King, and N. M. Laurendeau, "Measurements of hydroxyl concentrations and lifetimes in laminar flames using picosecond time-resolved laser-induced fluorescence," *Appl. Opt.* in review (1995).

(4) T. A. Reichardt, M. S. Klassen, G. B. King, and N. M. Laurendeau, "Measurements of hydroxyl concentrations and lifetimes in laminar flames using picosecond time-resolved laser-induced fluorescence," Spring Meeting, Central/Western States Section/The Combustion Institute, San Antonio, TX, 145 (1995).

(5) T. A. Reichardt, M. S. Klassen, G. B. King, and N. M. Laurendeau, "Correcting concentration measurements for quenching effects using picosecond time-resolved laser-induced fluorescence," Spring Meeting, Central States Section/The Combustion Institute, Madison, WI, 255 (1994).

(6) M. S. Klassen, T. A. Reichardt, G. B. King, and N. M. Laurendeau, "Correcting hydroxyl concentration measurements for quenching using picosecond time-resolved laser-induced fluorescence," Poster presented at the Twenty-fifth International Symposium on Combustion, The Combustion Institute, Pittsburgh, PA (1994).

(7) M. S. Klassen, T. A. Reichardt, G. B. King, and N. M. Laurendeau, "Flame concentration measurements using picosecond time-resolved laser-induced fluorescence," Poster presented at the Gordon Research Conference on the Physics and Chemistry of Laser Diagnostics in Combustion (1993).

(8) B. D. Thompson, G. B. King, and N. M. Laurendeau, "Flame concentration measurements using picosecond time-resolved laser-induced fluorescence," Spring Meeting, Central States Section/The Combustion Institute, Columbus, OH, 321 (1992).

4. RESEARCH PERSONNEL

Professors Galen B. King and Normand M. Laurendeau are co-principal investigators for this research. Dr. Michael S. Klassen joined the project in June, 1992 as a post-doctoral researcher. Mr. Thomas Reichardt, who also joined the project in June, 1992 obtained his M.S. degree in mechanical engineering in December, 1994. Mr. Brian Thompson completed his M.S. thesis in August, 1992.

REFERENCES

[1] Gupta, A. K. and Lilley, D. G. (1987). The gray areas in combustion research. *J. Inst. of Energy* **60**, 108.

[2] Crosley, D. R. (1981). Collisional effects on laser-induced fluorescence flame measurements. *Opt. Eng.* **20**, 511.

[3] Harris, J. M. and Lytle, F. E. (1977). Measurement of subnanosecond fluorescence decays by sampled single-photon detection. *Rev. Sci. Instrum.* **48**, 1469.

[4] Nowak, S. A., Basile, F., Kivi, J. T., and Lytle, F. E. (1991). Fast collection times for fluorescence-decay measurements. *Appl. Spectrosc.* **45**, 1026.

[5] Dieke, G. H. and Crosswhite, H. M. (1962). The ultraviolet bands of OH: fundamental data. *J. Quant. Spectrosc. Radiat. Transfer* **2**, 97.

[6] Garland, N. L. and Crosley, D. R. (1986). On the collisional quenching of electronically excited OH, NH and CH in flames. *Twenty-first Symposium (International) on Combustion*, The Combustion Institute, Pittsburgh, PA, 1693.

[7] Paul, P. H. (1994). A model for temperature-dependent collisional quenching of OH A^{2+}. *J. Quant. Spectrosc. Radiat. Transfer* **51**, 511.

[8] Cheng, T. S., Wehrmeyer, J. A., and Pitz, R. W. (1991). Laser Raman diagnostics in subsonic and supersonic turbulent jet diffusion flames. NASA Contractor Report 189544, p. 63.

[9] Kee, R. J., Grcar, J. F., Smooke, M. D., and Miller, J. A. (1985). A Fortran program for modeling steady laminar one-dimensional premixed flames. Sandia Report SAND85-8240.

[10] Kee, R. J., Rupley, F. M., and Miller, J. A. (1989). CHEMKIN-II: A Fortran chemical kinetics package for the analysis of gas-phase chemical kinetics. Sandia Report SAND89-

8009.

[11] Kee, R. J., Dixon-Lewis, G., Jr., Warnatz, J., Coltrin, M. E., and Miller, J. A. (1986). A Fortran computer code package for the evaluation of gas-phase multicomponent transport properties. Sandia Report SAND86-8246.

[12] Kee, R. J., Rupley, F. M., and Miller, J. A. (1987). A chemical thermodynamic data base. Sandia Report SAND87-8215.

[13] Barlow, R. S., Dibble, R. W., Chen, J. -Y., and Lucht, R. P. (1990). Effect of Damköhler number on superequilibrium OH concentration in turbulent nonpremixed jet flames. *Combust. Flame* **82**, 235.

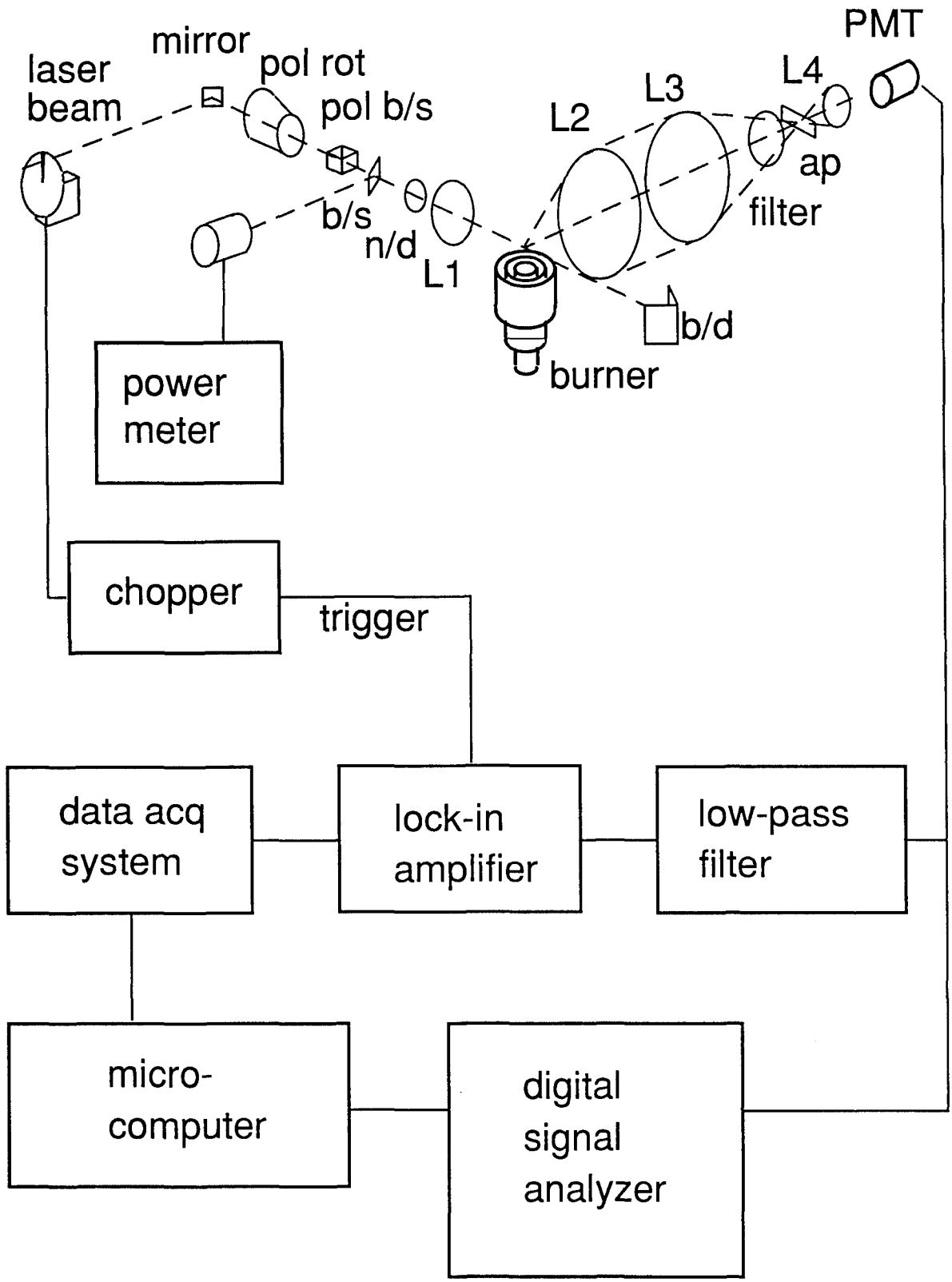

Figure 1. Schematic diagram of the experimental apparatus.

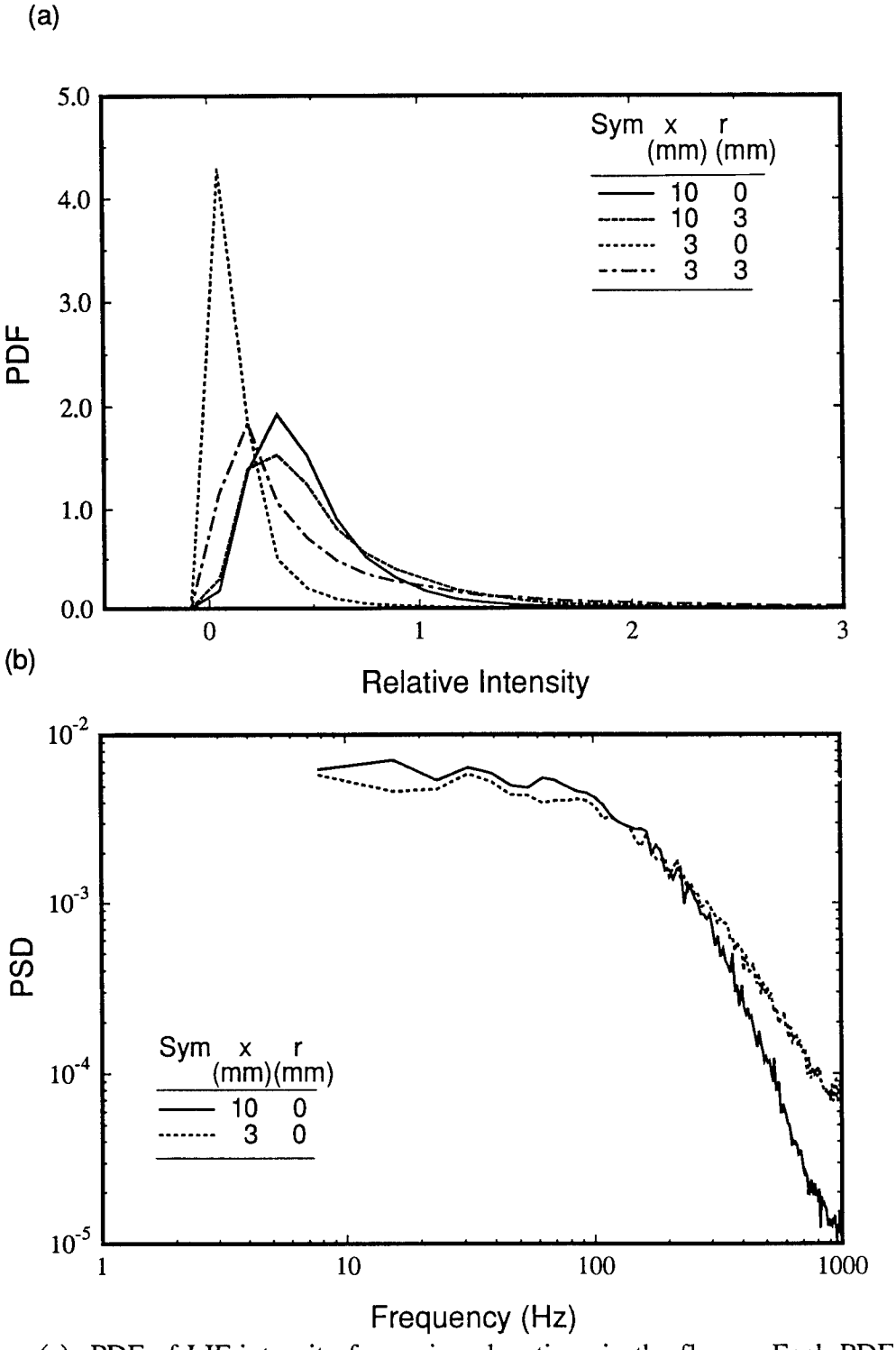

Figure 2. (a) PDF of LIF intensity for various locations in the flame. Each PDF is obtained from 25000 points sampled at 2 kHz. The average beam power used was 1 mW. (b) Normalized PSD of LIF intensity for two axial locations in the flame. Each PSD is obtained from 25000 points sampled at 2 kHz. The PSD is normalized by the mean-square of the LIF intensity fluctuations.

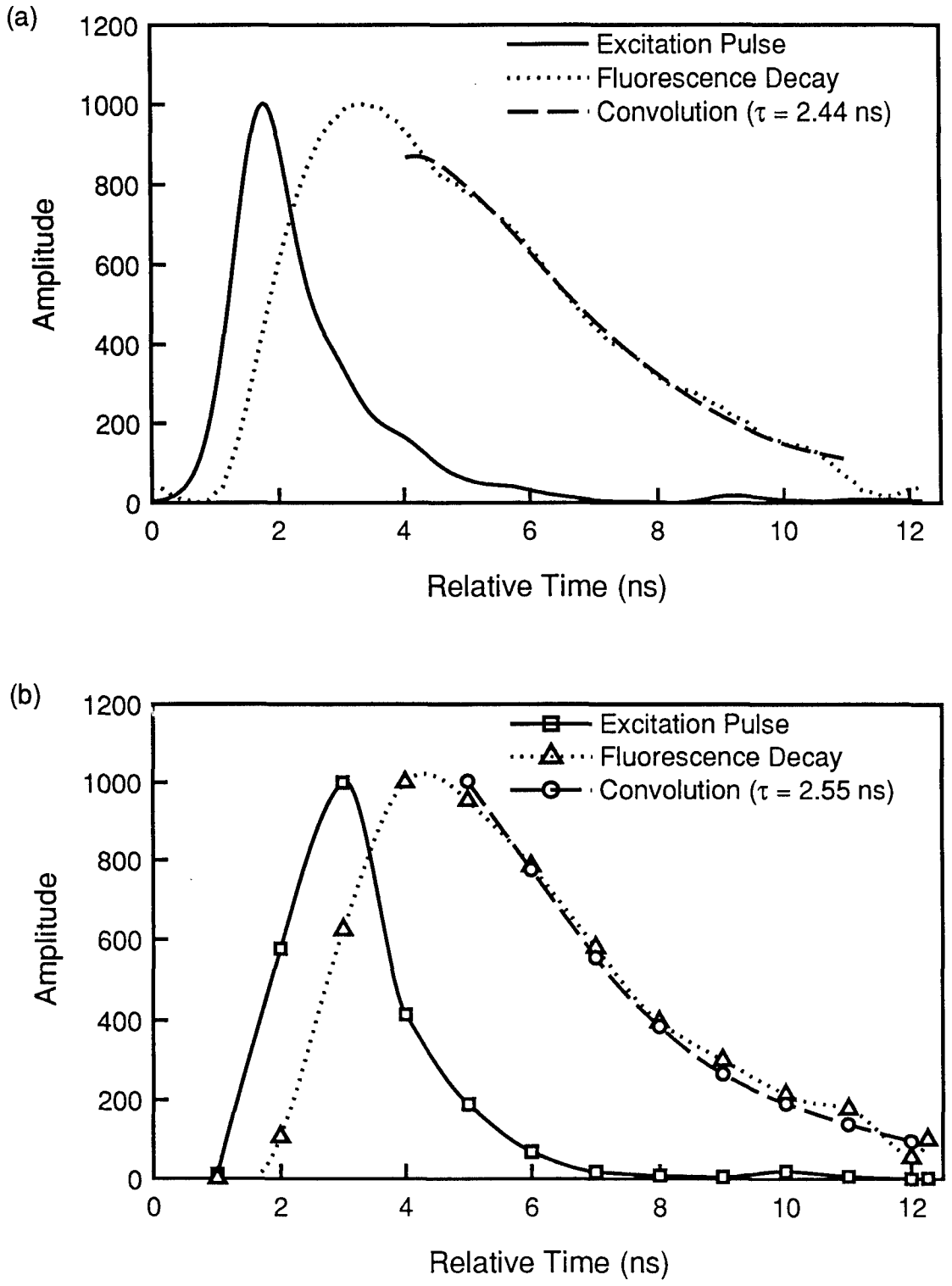

Figure 3. (a) Normalized equivalent-time excitation pulse and sodium fluorescence decay. The waveforms were smoothed using a digital n-pole Bessel filter with a risetime of 700 ps after averaging 500 equivalent-time waveforms. (b) Normalized real-time excitation pulse and sodium fluorescence decay reconstructed from 409 μs of data.

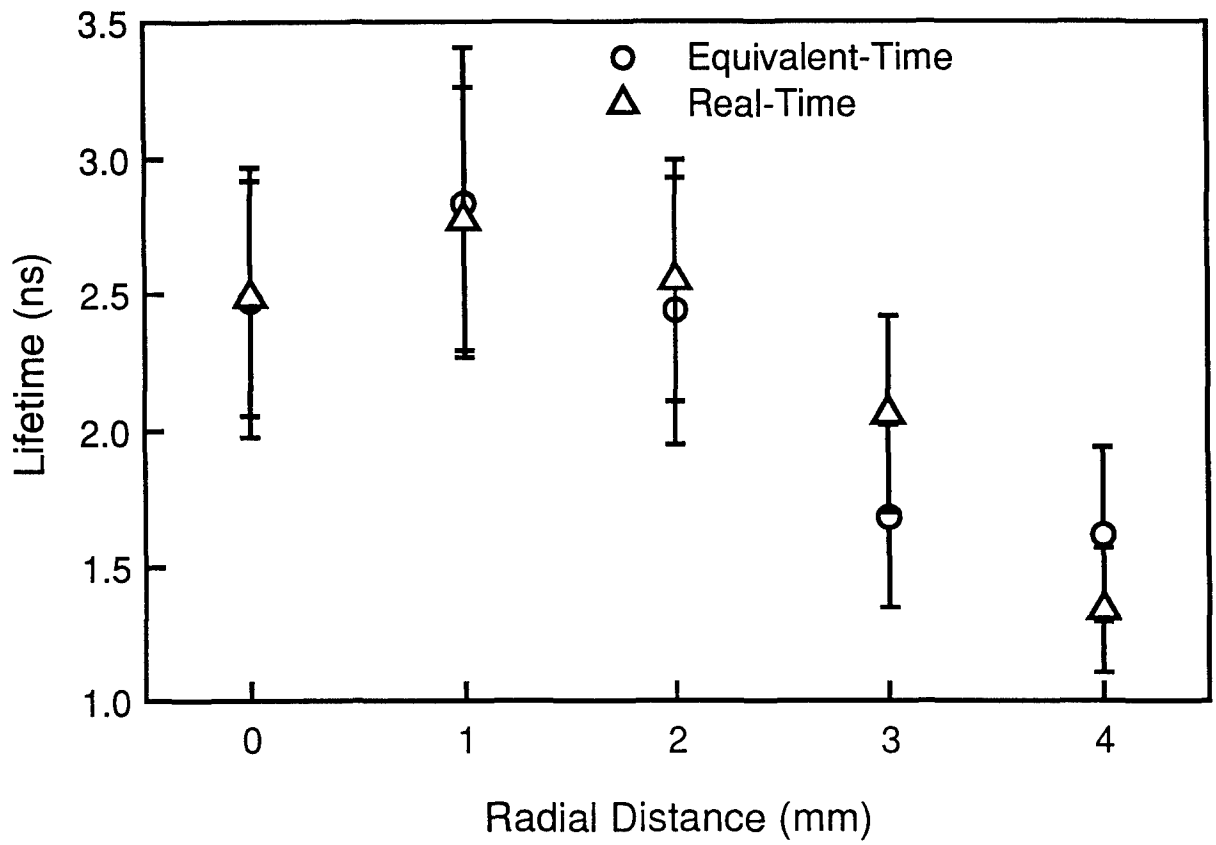

Figure 4. Quantitative comparison of equivalent-time and real-time measured sodium lifetimes as a function of position in the burner. The error bars indicate the $\pm 2\sigma$ intervals based on repeated trials using each technique.

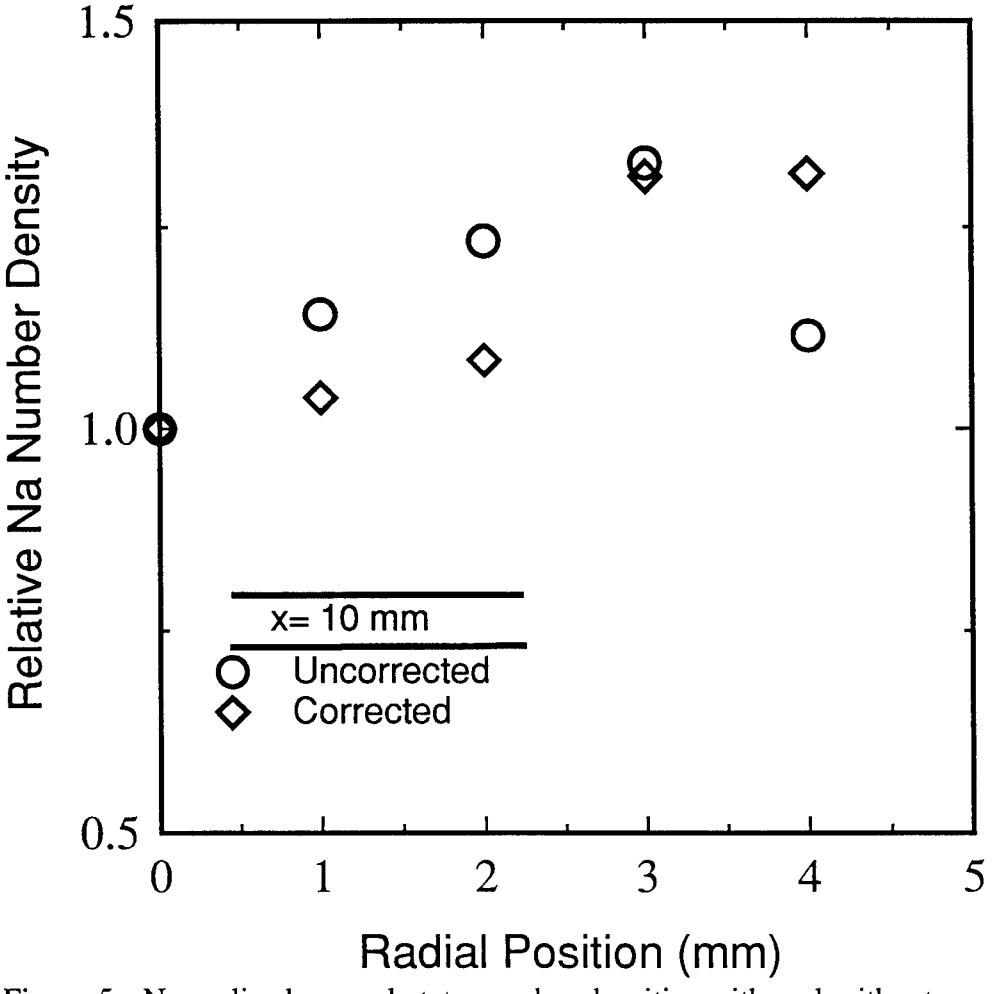

Figure 5. Normalized ground state number densities with and without correction for collisional quenching. The values for both the corrected and uncorrected number densities are normalized with respect to the corresponding value found at x=10 mm and r=0 mm.

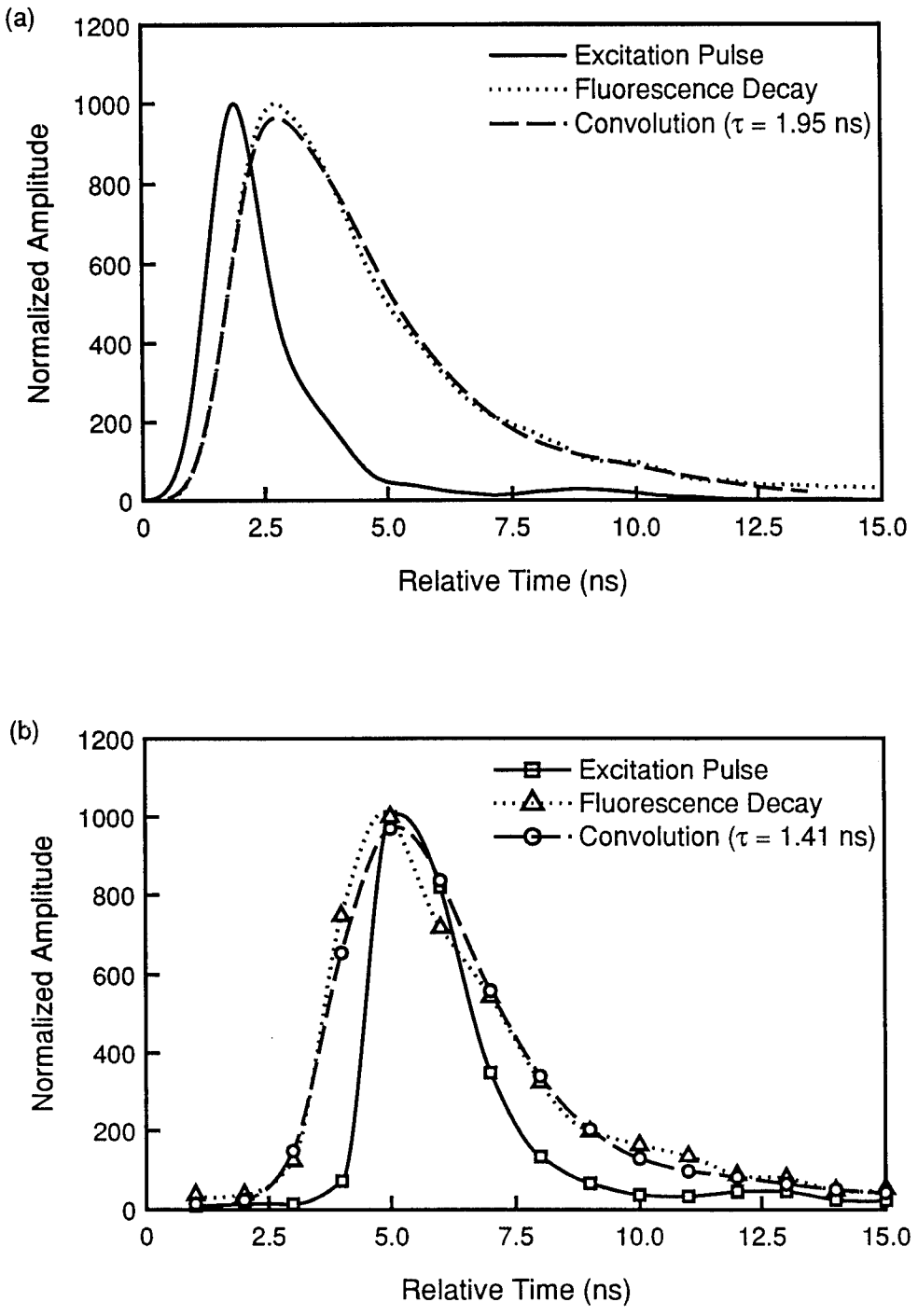

Figure 6. (a) Normalized equivalent-time instrument response and fluorescence decay obtained 5 mm above the center of the Hencken burner at ϕ=1.0. Both of these waveforms were obtained by averaging 500 individual waveforms and smoothing via a digital n-pole Bessel filter with a 900 ps risetime. (b) Similar normalized real-time waveforms obtained 5 mm over the McKenna burner at ϕ=1.0. The convolution of the excitation pulse with the exponential function determined from the convolute-and-compare algorithm is also displayed in both figures.

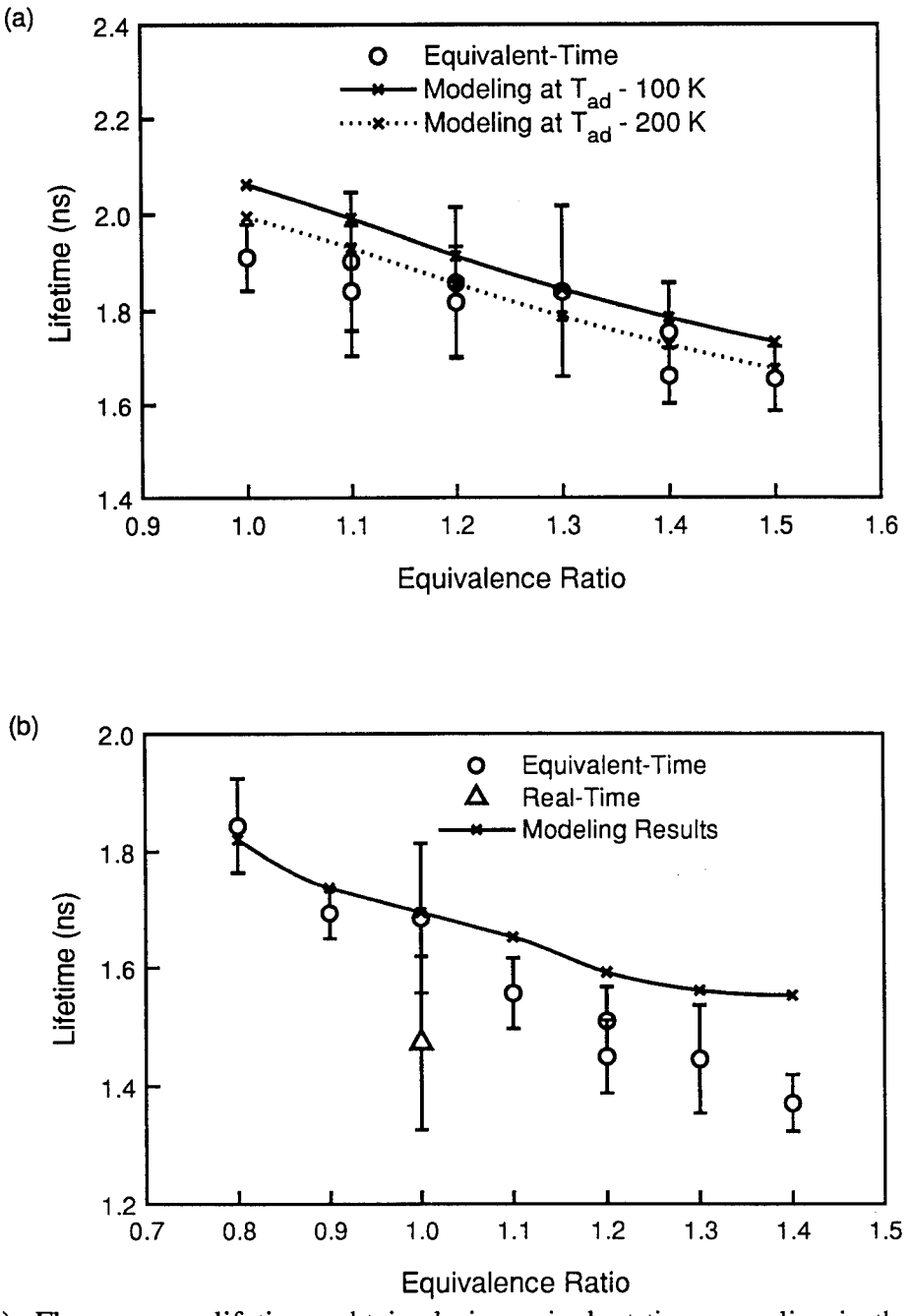

Figure 7. (a) Fluorescence lifetimes obtained via equivalent-time sampling in the center of the Hencken burner 5 mm above the burner surface. The fluorescence lifetimes obtained from the modeling are also displayed, assuming equilibrium conditions at temperatures 100 K below and 200 K below the adiabatic flame temperature. (b) Fluorescence lifetimes obtained via equivalent-time sampling in the center of the McKenna burner 5 mm above the burner surface. The result using real-time sampling is also included at ϕ=1.0. The fluorescence lifetimes obtained from modeling are also displayed. The mean lifetime and uncertainty ranges for all the lifetimes (95% confidence interval of the mean) are calculated from the results of six lifetime measurements.

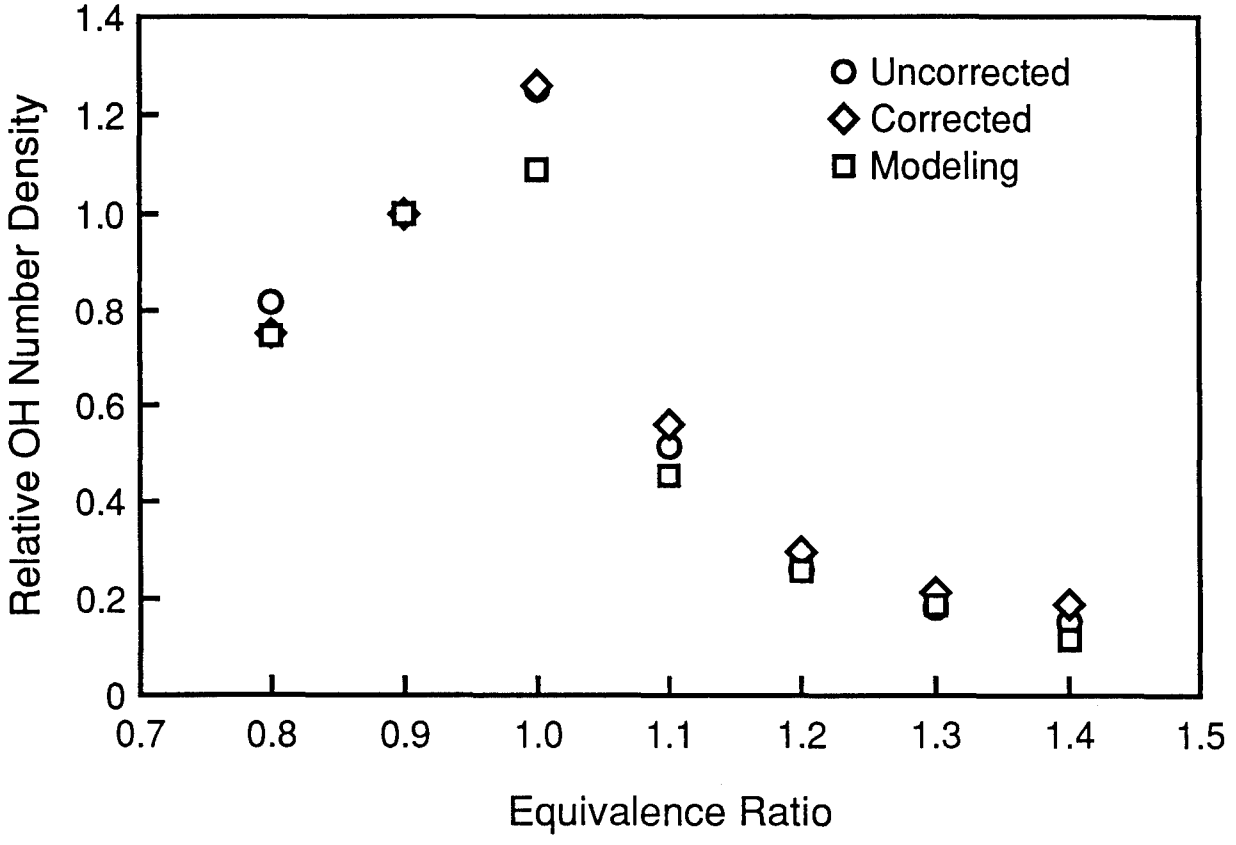

Figure 8. Normalized OH number densities 5 mm above the center of the McKenna burner for different equivalence rations with and without corrections for collisional quenching. The values for both the corrected and uncorrected number densities are normalized with respect to the corresponding value determined at ϕ=0.9.

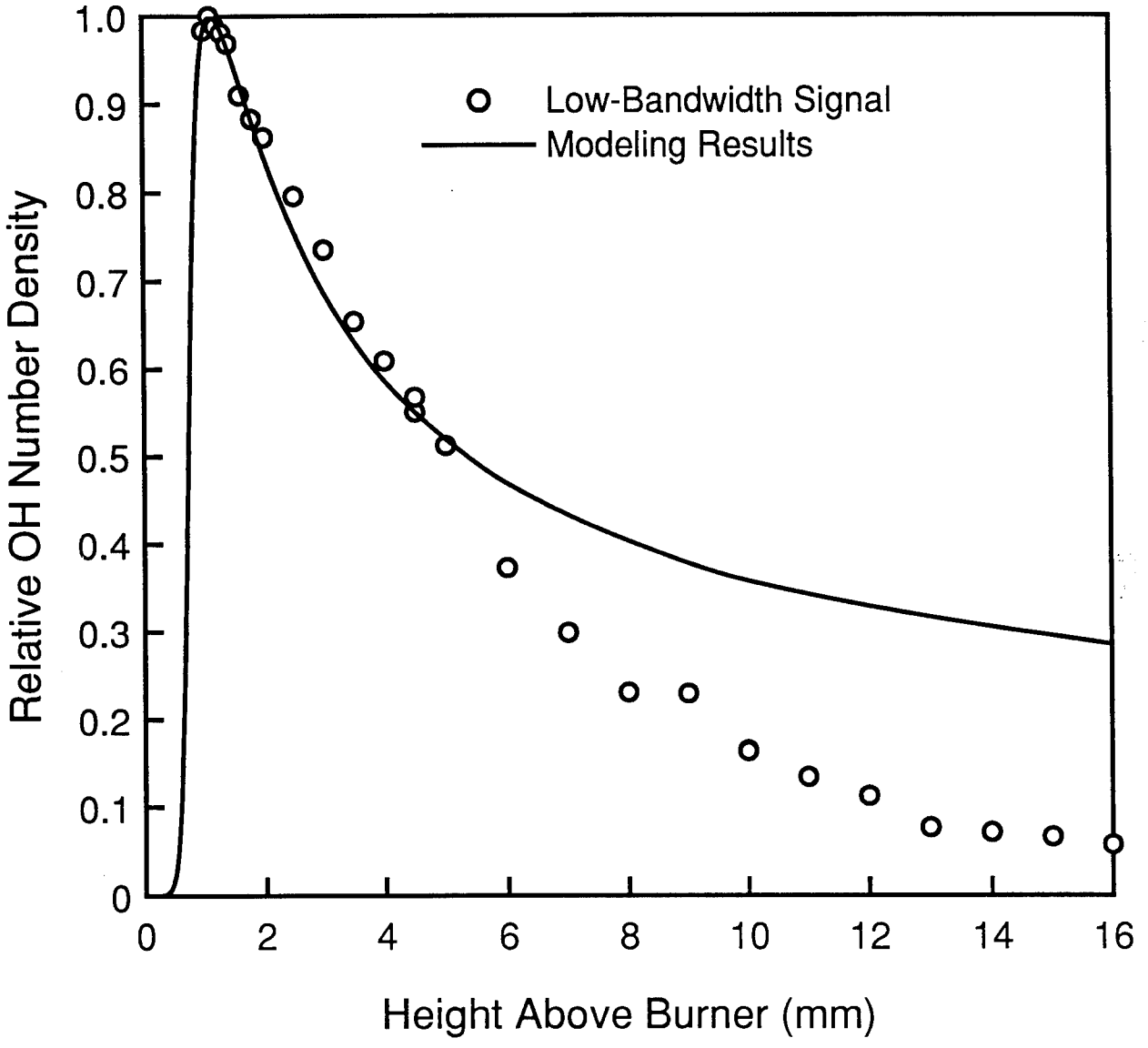

Figure 9. Axial profile of the low-bandwidth LIF signal. The relative OH signal is graphed versus height above the McKenna burner at ϕ=1.0. The results from kinetic modeling are also displayed.